# AJNR

**Microvascular Perfusion MRI Improves Therapy Monitoring and Detects Early Recurrences of Gliomas: A Large-Scale Trial of 2000 Follow-Up Examinations**

Andreas Stadlbauer, Katarina Nikolic, Franz Marhold, Arnd Doerfler, Thomas M. Kinfe, Anke Meyer-Bäse, Oliver Schnell, Alexandra Ökrösi, Gertraud Heinz and Stefan Oberndorfer

# Microvascular Perfusion MRI Improves Therapy Monitoring and Detects Early Recurrences of Gliomas: A Large-Scale Trial of 2000 Follow-Up Examinations

Andreas Stadlbauer, Katarina Nikolic, Franz Marhold, Arnd Doerfler, Thomas M. Kinfe, Anke Meyer-Bäse, Oliver Schnell, Alexandra Ökrösi, Gertraud Heinz, and Stefan Oberndorfer

## ABSTRACT

**BACKGROUND AND PURPOSE:** Detecting glioma recurrence is fundamental for clinical patient outcomes; however, conventional MRI (cMRI) techniques may be limited, leading to diagnostic uncertainty relevant for therapeutic intervention. This study aimed to evaluate whether a microvascular perfusion ($\mu$Perf) imaging technique based on spin-echo DSC perfusion MRI could support the early detection of glioma recurrence compared with cMRI by characterizing subtle vascular changes preceding macroscopic tumor growth.

**MATERIALS AND METHODS:** A total of 351 patients with gliomas who underwent 2003 follow-up MRI examinations were retrospectively evaluated, with 422 of these examinations subjected to detailed quantitative analysis. The standard cMRI protocol was extended by applying the $\mu$Perf approach, with an additional 2 minutes for data acquisition. Custom-made Matlab software was used to generate imaging biomarker maps for microvascular CBV and microvascular type indicator. The clinical utility of $\mu$Perf was assessed by comparing its findings with radiologic interpretations of cMRI data, which were reviewed in consensus by at least 2 board-certified radiologists. Statistical analyses included the calculation of diagnostic performance metrics and the area under the receiver operating characteristic curve (AUROC) to evaluate glioma recurrence detection.

**RESULTS:** The $\mu$Perf technique exhibited superior diagnostic performance, achieving an accuracy of 97.4% and AUROC values of 0.987 (95% CI, 0.976–0.999) for microvascular type indicator and 0.982 (95% CI, 0.965–0.998) for microvascular CBV, significantly surpassing cMRI (accuracy: 85.1%; AUROC: 0.941; 95% CI, 0.918–0.965 for CBV). $\mu$Perf identified glioma recurrence earlier than cMRI in 13.5% of cases, with the time interval ranging from 41 to 353 days (mean, 137 days). During this time, tumor volume increased by 38% to as much as 155-fold (mean, 9.1-fold). Notably, early recurrences of high-grade malignant gliomas were predominantly characterized by microvascular changes compared with later-stage recurrences.

**CONCLUSIONS:** $\mu$Perf improves early detection of glioma recurrence and shows a higher sensitivity of microvascular changes compared with cMRI. $\mu$Perf has significant potential to promote more timely and personalized treatment strategies, which, in turn, could improve patient outcomes. Notably, $\mu$Perf works with standard clinical follow-up protocols, but its integration into clinical practice requires further validation through multicenter studies and long-term outcome analyses.

**ABBREVIATIONS:** AUROC = area under the ROC curve; cMRI = conventional MRI; cNWM = contralateral normal-appearing white matter; ceT1w = post-contrast-enhanced T1-weighted; FET = [$^{18}$F]-fluoroethyl-tyrosine; FN = false-negative; FP = false-positive; GBM = glioblastoma; MTI = microvascular type indicator; $\mu$CBV = microvascular CBV; $\mu$Perf = microvascular perfusion; ROC = receiver operating characteristic; TN = true-negative; TP = true-positive; WHO = World Health Organizaton; RANO = Response Assessment in Neuro-Oncology

G liomas represent a heterogeneous group of solid brain neoplasms representing a clinical challenge due to their infiltrative nature and high recurrence rates. Glioblastoma (GBM)

## SUMMARY

**PREVIOUS LITERATURE:** Recent studies have highlighted the challenges in distinguishing between glioma recurrence and treatment-related changes by using cMRI techniques, such as contrast-enhanced T1-weighted MRI, DWI, and gradient-echo–based DSC perfusion MRI. Meta-analyses reported sensitivities and specificities for cMRI of 83%–90% and 87%–94%, respectively, for detecting high-grade glioma recurrence. Advanced imaging modalities like amino acid PET and multiparametric approaches combining PET with perfusion MRI have shown improved diagnostic accuracy, with AUROC values up to 0.98.

**KEY FINDINGS:** Microvascular perfusion imaging using spin-echo DSC MRI outperformed cMRI in the early detection of glioma recurrence, showing higher accuracy (97.4%) and AUROC (>0.98), with earlier detection in 13.5% of cases and easy integration into routine protocols.

**KNOWLEDGE ADVANCEMENT:** This study demonstrated that microvascular perfusion imaging increased the sensitivity for microvascular changes, allowing earlier and more accurate detection of glioma recurrence than cMRI. This result supports its integration into standard protocols and RANO updates.

World Health Organization (WHO) grade 4, *IDH* wild-type) is the most prevalent primary brain tumor in adults, associated with a poor prognosis and characterized by a median overall survival of just 15–18 months, and a 5-year survival rate of <5%.[1] Glioma WHO grade 3 is another highly aggressive form of primary brain tumor that often affects young adults in the prime of their lives and is associated with severe disability and ultimately death.[2] In contrast, glioma WHO grade 2 are slower-growing tumors that tend to have a more prolonged clinical course yet tend to progress into higher-grade malignancies.[3]

Despite advances in the treatment of glioma—surgery, radiation therapy, and chemotherapy—the prognosis, especially for patients with GBM, has remained poor in recent decades. A major reason is that treatment failure and recurrence are still inevitable, particularly in high-grade gliomas.[4] Early detection of tumor recurrence is crucial for timely intervention, because it can significantly impact patient prognosis and treatment outcomes.[5] However, differentiating recurrence from treatment-related changes, such as radiation necrosis, remains a diagnostic hurdle in clinical neuro-oncology.

MR imaging is the standard imaging technique for monitoring gliomas. However, even advanced MRI techniques, such as DWI and PWI MRI have weaknesses in differentiating between tumor progression and pseudoprogression, which, in turn, leads to delays in diagnosis and treatment intervention.[6] These limitations underscore the urgent need for innovative imaging protocols with the ability to improve the reliability in the detection of glioma recurrence to counterbalance the uncertainty in identifying glioma recurrence, which, to date, necessitates repeat follow-up examinations. In conventional MRI (cMRI) protocols, the DSC technique with gradient-echo sequences is used. However, previous studies have shown that the vessel-size sensitivity of the gradient-echo DSC signal has a plateau down to a vessel radius of about 10 $\mu$m and decreases markedly at smaller-vessel radii.[7,8]

Microvascular perfusion ($\mu$Perf) extends the conventional perfusion mapping by incorporating spin-echo DSC measurements, and unlike the gradient-echo DSC signals, spin-echo DSC signals demonstrate a peak sensitivity to the microvasculature at a vessel radius of approximately 5 $\mu$m,[7,8] encompassing capillaries as well as small arterioles and venules. Early-stage neovascularization is characterized by very thin vascular structures,[9] which are difficult to detected using conventional gradient-echo DSC perfusion MRI used in cMRI protocols.

Our hypothesis was that by leveraging high-resolution imaging of microvascular perfusion and neovascularization, we can increase the diagnostic yield of early glioma recurrence detection by identifying subtle vascular changes at an early stage.

This study investigated the clinical utility of $\mu$Perf in the early detection of glioma recurrences by comparing $\mu$Perf parameters such as microvascular CBV ($\mu$CBV) and microvascular type indicator (MTI) with cMRI data. The aim was determining whether $\mu$Perf can offer improved diagnostic reliability in identifying recurrent tumors. Additionally, we explored the potential of $\mu$Perf to provide insights into the underlying pathophysiological processes of glioma recurrence, with the goal to establish personalized management strategies.

## MATERIALS AND METHODS
### Patient Selection
A consecutively and prospectively populated institutional database was reviewed to identify patients with glioma who underwent follow-up MRI examinations between July 2015 and June 2024 after receiving standard-of-care treatments. These treatments included maximal safe resection, radiation therapy, and both concomitant and adjuvant chemotherapy with temozolomide.

The inclusion criteria for this study were as follows: 1) patients older than 18 years of age; 2) histopathologic confirmation of adult-type diffuse glioma according to the WHO Classification of Tumors of the CNS;[10] 3) availability of data from the study MRI protocol from ≥1 follow-up examination; and 4) interpretation of cMRI data from the clinical routine by at least 2 board-certified radiologists in consensus.

A total of 351 patients (148 women, 203 men; mean age, 57.5 [SD, 13.7] years; age range, 19.2–85.3 years) met these criteria, resulting in a total of 2003 follow-up MRI examinations being retrospectively re-evaluated for this study (on average, 5.7 per patient). The number of follow-up MRI examinations per patient ranged between 1 and 25. The institutional review boards of the University Clinic of St. Pölten and the University of Erlangen approved this retrospective research. All patients provided written informed consent in accordance with the ethical standards outlined in the Helsinki Declaration of 1975 and its subsequent amendments.

## MRI Data Acquisition

Follow-up MRI examinations were conducted at intervals of 3–6 months for high-grade gliomas (WHO grades 3 and 4) and 6–12 months for low-grade gliomas (WHO grade 2) or on an unscheduled basis if clinical signs of tumor recurrence were observed. MRI data acquisition was performed using a clinical 3T scanner (Magnetom Trio; Siemens) equipped with a standard 12-channel head coil.

The MRI protocol included, among others, the following sequences in the order of execution: 1) a FLAIR sequence; 2) a DWI sequence ($b = 0$, 1000, and 2000 s/mm$^2$); 3) for MRI-based investigation of $\mu$Perf, a DSC perfusion MRI using a spin-echo EPI sequence (TR = 1740 ms, TE = 33 ms, flip angle = 90°, refocusing angle = 180°); 4) a DSC perfusion MRI sequence using gradient-echo EPI (TR = 1740 ms, TE = 22 ms, flip angle = 90°), requiring a separate injection of contrast agent; and 5) pre- and postcontrast-enhanced T1-weighted (ceT1w) imaging. All sequences were acquired in an axial orientation.

Both DSC sequences included 60 dynamic measurements with 0.1 mmol/kg of gadoterate meglumine (Dotarem; Guerbet) administered at a rate of 4 mL/s using an MR-compatible injector (Spectris; Medrad).

The spin-echo DSC perfusion MRI was performed before the gradient-echo DSC perfusion MRI, which is beneficial in 2 ways because the spin-echo EPI technique is less sensitive to contrast agent leakage[11] and the first contrast agent injection for the spin-echo DSC perfusion MRI acts as a prebolus for leakage artifact reduction of the more leakage-sensitive gradient-echo DSC perfusion MRI (preload contrast agent leakage-correction approach).[12,13] Strategies to minimize patient motion and variations in the timing of the first-pass peak—factors that could significantly influence data evaluation—were previously described.[14] Identical geometric parameters were maintained for both DSC sequences, including an in-plane resolution of 1.8 × 1.8 mm, slice thickness of 4 mm, 29 slices, and a generalized autocalibrating partially parallel acquisition (GRAPPA) factor of 2. The additional acquisition time required for the spin-echo DSC perfusion sequence was approximately 2 minutes.

## MRI Data Analysis

Processing of cMRI data involved calculating maps of ADC from DWI data. The postprocessing of the perfusion data was performed using the method described by Bjørnerud and Emblem[15] for the fully-automated quantitative cerebral hemodynamic analysis of DSC-MRI data by calculating CBV maps through automatic identification of arterial input functions. Interpretation of cMRI data—including DWI and CBV maps—was performed by 2 board-certified radiologists in consensus according to the updated Response Assessment in Neuro-Oncology (RANO) criteria for detecting glioma recurrence and without inclusion of $\mu$Perf data.

Processing $\mu$Perf data used custom Matlab software (MathWorks) and included the calculation of maps for $\mu$CBV and the MTI. The $\mu$CBV maps were generated from the spin-echo DSC perfusion data alone via a separate automatic identification of arterial input functions.[15] The concept behind the MTI maps involved the combined evaluation of the 2 perfusion MRI sequences. This required, as a first step, the construction of the so-called vascular hysteresis loop diagrams ($\Delta R_{2,\text{gradient-echo}}$ versus ($\Delta R_{2,\text{spin-echo}})^{3/2}$),[16] achieved by fitting the initial contrast agent bolus curves from both gradient-echo and spin-echo DSC perfusion data by using a previously established gamma-variate function.[17] Next, the MTI parameter was calculated as the area of the vascular hysteresis loop, with its rotational direction determining the sign: Clockwise VHLs received a positive sign, while counterclockwise VHLs were assigned with a negative sign.

According to prior studies,[14] a positive MTI value indicates an arteriolar-dominated vascular system, while negative values suggest venule- and capillary-like components. In MTI maps, warm colors represented positive values, while cool colors indicated negative values. Thus, these maps differentiated between supplying arterial microvasculature and draining capillary-venous structures.[14] Furthermore, more negative MTI values indicated heightened neovascularization activity within tumors.[18]

## Statistics

For quantitative analysis, ROIs were manually defined in areas of contrast enhancement on ceT1w images and hyperintensities on FLAIR images suspected of tumor recurrence by a radiologist, neuro-oncologist (neurologist or neurosurgeon), and an MR physicist in consensus. Additional ROIs were placed in contralateral normal-appearing white matter (cNWM) for internal reference. Imaging biomarker values for CBV, $\mu$CBV, and MTI were calculated for these ROIs.

Patient subgroups were retrospectively categorized according to imaging features observed in both cMRI and $\mu$Perf data across all follow-up examinations during the study period: true-positive (TP), false-positive (FP), true-negative (TN), and false-negative (FN) results for glioma recurrence detection. Diagnostic performance parameters such as sensitivity, specificity, precision, accuracy, and F1 score were derived from the confusion matrix (Supplemental Data). Tumor volumes were also measured on ceT1w or FLAIR images for patients with recurrence. All data were expressed as mean (SD).

Statistical evaluation was conducted using dedicated software (SPSS; IBM). Differences in imaging biomarkers between patient subgroups were analyzed using the general linear model. The Dunnett-T3 test served as a post hoc procedure to address potential violations of variance homogeneity assumptions while correcting for multiple comparisons. Homogeneity was assessed via the Levene test.

Intraindividual differences in imaging biomarker values between lesions and cNWM, as well as tumor volume changes across follow-up examinations, were compared using Wilcoxon signed-rank tests. The significance of tumor volume differences among patient subgroups was evaluated using Mann-Whitney $U$ tests. A $P$ value $< .05$ was considered significant. Receiver operating characteristic (ROC) analysis was conducted to compute the area under the ROC curve (AUROC), providing insights into the diagnostic performance of each imaging biomarker for detecting glioma recurrence. We followed methodology proposed in the TRIPOD checklist (Supplemental Data).

## RESULTS

### Patients

Of the 2003 follow-up MRI examinations performed in 351 patients as part of this study, 422 examinations (21.1%) were

```
Institutional brain tumor MRI database
Jul 2015 – Jul 2024
(n = 803; 2605 exams)
                    │
                    │ excluded ──────────▶  Histopathology other
                    │                        than glioma
                    │                        (n = 273; 367 exams)
                    ▼
Glioma
WHO grade 2 – 4
(n = 530; 2238 exams)
                    │
                    │ excluded ──────────▶  Standard of care
                    │                        treatments not
                    │                        completed;
                    │                        or
                    │                        Histopathology not
                    │                        available
                    │                        (n = 179; 235 exams)
                    ▼
Study Data
Follow-up MRIs
Glioma
WHO grade 2 – 4
(n = 351; 2003 exams /
422 suspicious exams)
                    │
                    │  ────────────────▶  No Recurrence during
                    │                      the study period
                    │                      (n = 66; 81 exams)
                    ▼                      cMRI: 76 TN; 5 FP
Recurrence of the                          µPerf: 77 TN; 4 FP
Glioma
(n = 285; 341 exams)
         │           │            │
         ▼           ▼            ▼
Consistent result  Early detection  Recurrence
in cMRI & µPerf    in µPerf         without µPerf
cMRI: 277 TP; 1 FN cMRI: 57 FN      cMRI: 6 TP
µPerf: 277 TP; 1 FN µPerf: 57 TP    µPerf: 6 FN
```
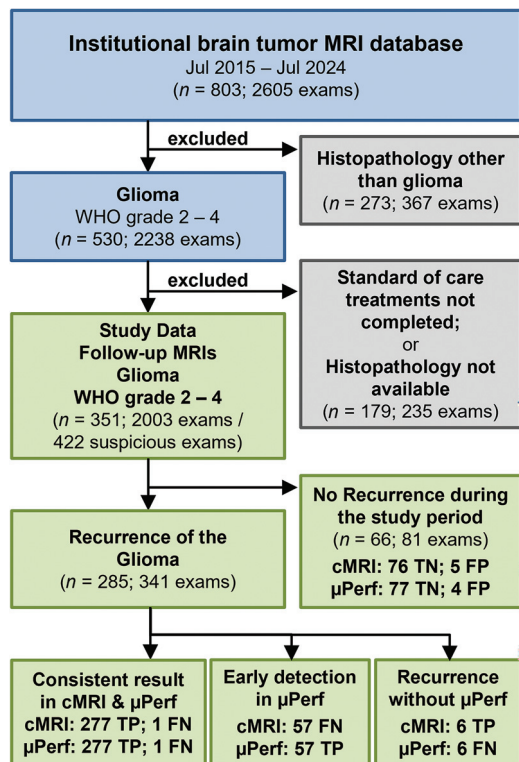
**FIG 1.** The flow diagram summarizes the patient selection protocol including exclusion criteria (gray boxes) and visualizes the definition of diagnostic subgroups analyzed in the study (green boxes), including the number of patients (n) and MRI examinations (examinations) as well as the predicted cMRI and $\mu$Perf findings.

subjected to detailed quantitative analysis because at least one of the cMRI data sets showed suspicious alterations that could indicate recurrence or progression. Among these 422 follow-up examinations, glioma recurrence was present in 341 examinations of 285 patients, whereas in 81 examinations of 66 patients, there was no recurrence during the study period of 108 months. A flow chart for patient selection is shown in Fig 1.

The patient-related number of recurrences was the following: Two hundred thirty-nine patients showed a single recurrence of the glioma during the observed course of the disease, 37 patients had a recurrence twice, 8 patients had a recurrence 3 times, and 1 patient had a recurrence of the glioma 4 times during the study period. All recurrences represented separate recurrences.

Treatment of recurrence was initiated in a weekly interdisciplinary tumor board meeting according to clinical symptoms and taking into account cMRI data: Seventy-four recurrences (21.7%) were treated by repeat craniotomy (35 in combination with additional radiation therapy and/or chemotherapy), and 88 recurrences (25.8%) were treated by second-line monotherapy with the antiangiogenic drug bevacizumab. Repeat radiation therapy or combined radiochemotherapy was initiated in 61 cases (17.9%), a temozolomide rechallenge was performed in 49 cases (14.4%), lomustine was administered in 19 cases (5.6%), and more experimental therapies (imatinib, nivolumab, osimertinib, pembrolizumab, and PCV—the combination of procarbazine, lomustine, and vincristine) were chosen in 10 cases (2.9%). Forty patients (11.7%) received palliative care without further treatment

of the tumor. Patient characteristics and clinical data are summarized in the Supplemental Data.

### Detection of Glioma Recurrence with cMRI and $\mu$Perf
**Suspicious Follow-Up MRIs without Recurrence.** Of the 81 examinations in 66 patients with suspicious changes that turned out not to be recurrences or progressions, 75 cMRI and $\mu$Perf examinations consistently yielded the correct result (TN) (Supplemental Data). In 2 follow-up examinations, the cMRI finding was FP, but the $\mu$Perf finding was TN (Supplemental Data). Conversely, in 1 examination, cMRI was TN, while $\mu$Perf was FP (Supplemental Data). Finally, 3 examinations consistently had a FP result in both cMRI and $\mu$Perf (Supplemental Data). This result produced a total of 76 TN and 6 FP findings for the cMRI, and 77 TN and 4 FP results for $\mu$Perf. In all FP cases, no recurrence treatment was initiated, because clinical parameters showed no evidence of recurrence. Subsequent follow-up examinations of these patients (ranging from 2 to 13 examinations during 11 months to 5 years) confirmed no evidence of recurrence.

**Follow-Up MRIs with the Same Finding in cMRI and $\mu$Perf.** Among the 341 examinations of 285 patients with an actual recurrence, a consistent TP result in cMRI and $\mu$Perf was observed in 277 examinations of 239 patients. Figure 2 shows exemplary cases of recurrence of an initial astrocytoma (WHO grade 2, *IDH*-mutated) and a GBM (WHO grade 4, *IDH*-wild-type), respectively. In one case (oligodendroglioma WHO grade 2, *IDH*-mutant, 1p19q codeleted), the follow-up examination consistently revealed a FN result in both cMRI and $\mu$Perf (Supplemental Data).

**Early Glioma Recurrence Detection with $\mu$Perf.** In 57 examinations of 55 patients with glioma recurrence, the $\mu$Perf data showed a TP result, whereas the cMRI findings were FN, indicating that in 13.5% of the detailed follow-up MRIs, glioma recurrence was detected earlier with $\mu$Perf than with cMRI. However, recurrence was subsequently diagnosed by cMRI in 28 cases during the next follow-up and in 7 cases during the second follow-up examination. In the remaining 22 cases, therapy was initiated despite FN cMRI findings. Illustrative cases are shown in Fig 3. In the first patient, recurrence of the GBM was detected by $\mu$Perf 67 days prior (Fig 3A) to its detection by cMRI (Fig 3B). During this time, the recurrent tumor volume increased from 6.8 to 102.1 cm$^3$, corresponding to a 14-fold increase. In the second example (Fig 3C), the treating physician initiated treatment with bevacizumab on the basis of the $\mu$Perf results, despite negative cMRI findings. An example of a patient whose recurrence was diagnosed only during the second follow-up (224 days later) using cMRI data is shown in the Supplemental Data. In all these cases, posttherapeutic effects were diagnosed due to the lack of hyperperfusion in conventional gradient-echo DSC perfusion MRI.

The average time differences between the early TP $\mu$Perf findings and the subsequent (delayed) TP cMRI follow-up examinations for all 55 patients were 137 [SD, 77] days (range, 41–353 days). During this time, tumor volumes increased significantly ($P < .001$) from 13.4 [SD, 8.8] cm$^3$ (0.2–100.1 cm$^3$) to 30.6 [SD, 29.2] cm$^3$ (1.0–118.0 cm$^3$) (Fig 4). The degree of tumor volume increase ranged
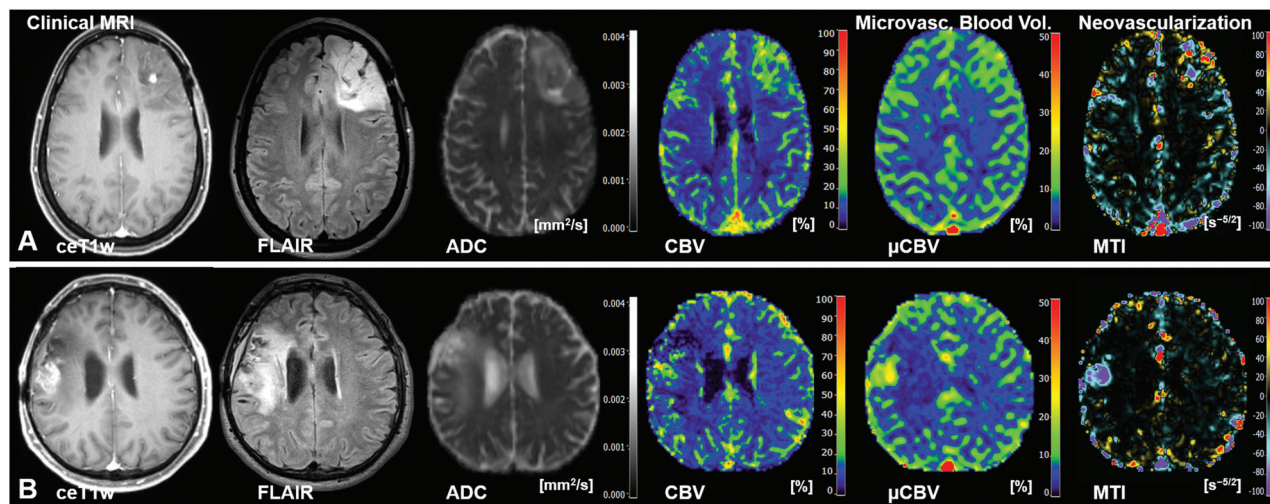
**FIG 2.** Consistent TP results in cMRI and $\mu$Perf for glioma recurrences. *A*, cMRI including anatomic sequences (ceT1w and FLAIR), diffusion-weighted (ADC), and macrovascular perfusion (CBV) MRI as well as $\mu$Perf biomarker maps of $\mu$CBV and MTI of a 40-year-old female patient with an astrocytoma WHO grade 2 (*IDH*-mutated) showing recurrence and malignant transformation. This patient received repeat combined radio-chemotherapy. *B*, cMRI and $\mu$Perf biomarker maps of a 63-year-old male patient with recurrent GBM (WHO grade 4, *IDH* wild-type). This patient underwent re-craniotomy followed by a repeat combined radiochemotherapy. In both cases, areas of increased macrovascular perfusion, microvascular perfusion, and neovascularization are clearly visible. Microvasc. indicates microvascular; Vol., volume.
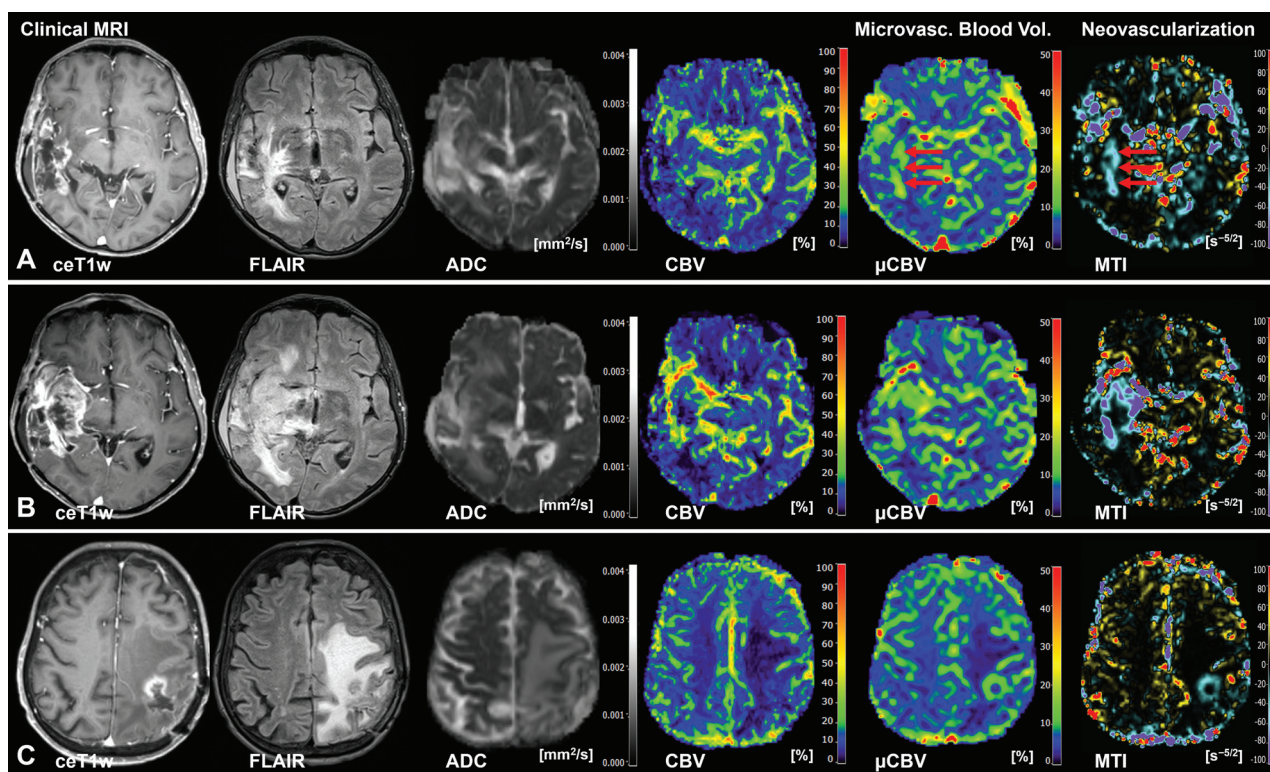


**FIG 3.** Early TP detection of glioma recurrence with $\mu$Perf and FN findings in cMRI. *A*, cMRI including anatomic sequences (ceT1w and FLAIR), diffusion-weighted (ADC), and macrovascular perfusion (CBV) MRI as well as $\mu$Perf biomarker maps of $\mu$CBV and neovascularization (MTI) of a 66-year-old female patient with a GBM who was diagnosed with "posttherapeutic effects, no signs of recurrence" in cMRI due to lack of macrovascular hyperperfusion in CBV. $\mu$Perf data, however, showed evidence of recurrence (*red arrows*), ie, microvascular hyperperfusion in $\mu$CBV and an indication of neovascularization in MTI at the initial follow-up examination. *B*, At the subsequent follow-up examination 67 days later the patient shows clear signs of recurrence in cMRI data, and progression of the recurrent GBM in $\mu$Perf data. The tumor volume had increased 14-fold, from 6.8 to 102.1 cm$^3$ within the 67 days. The patient received bevacizumab as second-line monotherapy due to clinically confirmed tumor progression. *C*, cMRI and $\mu$Perf biomarker maps of a 68-year-old male patient with GBM (WHO grade 4, *IDH* wild-type). The cMRI data were classified as radiation necrosis and pseudoprogression due to lack of macrovascular hyperperfusion in CBV. Signs of increased microperfusion and neovascularization are clearly visible. Despite negative cMRI findings, the treating physician initiated therapy with bevacizumab. Microvasc. indicates microvascular; Vol., volume.
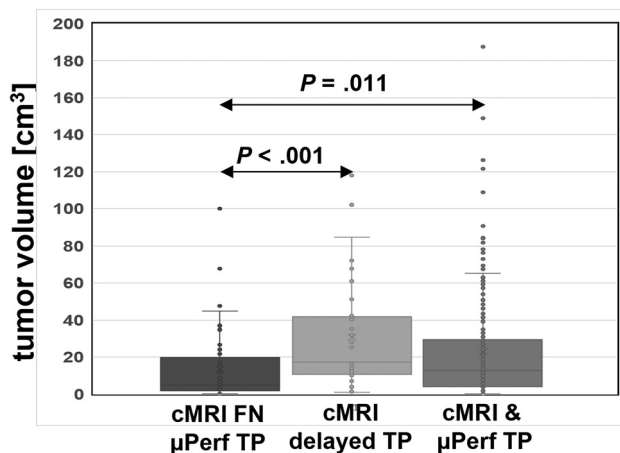
**FIG 4.** Tumor volumes for the diagnostic subgroups with an FN finding in cMRI data and a TP result for μPerf data, ie, early recurrence detection with μPerf (*dark gray box-and-whisker plot* on the left). The corresponding tumor volumes of the same patients at the subsequent follow-up with delayed TP findings in cMRI are depicted as a *light gray box-and-whisker plot* in the center. In other words, during the time of early recurrence detection with μPerf and delayed radiologic recurrence detection by routine cMRI, the tumor volumes increased significantly. The *gray box-and-whisker plot* on the right depicts the tumor volumes for the diagnostic subgroup with consistent TP findings in both cMRI and μPerf data.

from 38% to 155-fold (9.1-fold on average). The tumor volume values are summarized in the Supplemental Data.

The initial histopathology of gliomas detected earlier by μPerf was as follows: 37 glioblastomas WHO grade 4, *IDH*-wild-type (67.3%); 4 diffuse astrocytomas *IDH*-wild-type, NOS (7.3%); 3 *IDH*-mutant astrocytomas WHO grade 4 (5.5%); 2 *IDH*-mutant astrocytomas WHO grade 3 (3.6%); 1 *IDH*-mutant astrocytoma WHO grade 2 (1.8%); 7 oligodendrogliomas WHO grade 3, *IDH*-mutant, 1p19q codeleted (12.7%); and 1 oligodendroglioma WHO grade 2, *IDH*-mutant, 1p19q codeleted (1.8%). The high proportion of oligodendrogliomas WHO grade 3, *IDH*-mutant, 1p19q codeleted is noteworthy, because this group comprised only 6.8% of the entire patient cohort (Supplemental Data).

**Recurrence without Signs of Microperfusion.** In 6 patients, cMRI data were evaluated as TP, while μPerf data provided FN results. This finding indicates recurrence of gliomas without signs of microperfusion or neovascularization. Of these cases, 2 gliomas were astrocytoma WHO grade 2, *IDH*-mutant, and 1 glioma was a diffuse astrocytoma *IDH*-wild-type NOS that recurred without malignant transformation. However, 3 tumors were GBMs that showed no signs of increased microperfusion or neovascularization (Supplemental Data).

### Diagnostic Performance and Quantitative Imaging Biomarker Evaluation

The elements of the confusion matrix for glioma recurrence detection with cMRI were the following: TN = 76, FP = 5, TP = 283, and FN = 58. For glioma recurrence detection with μPerf, the corresponding values were TN = 77, FP = 4, TP = 334, and FN = 7. The confusion matrices are summarized in the
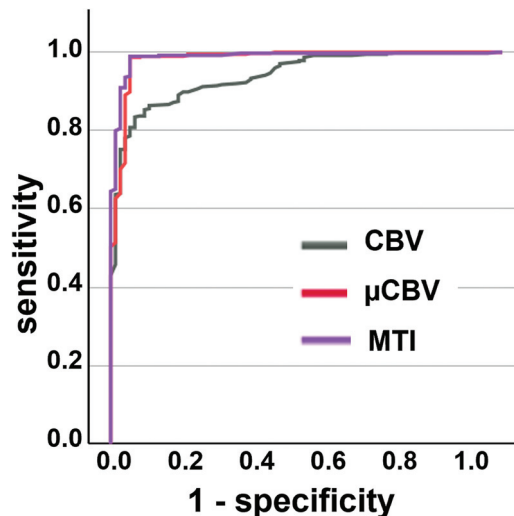


**FIG 5.** ROC curve analysis illustrates the diagnostic performance for glioma recurrence detection of cMRI (CBV) and μPerf biomarkers (μCBV and MTI). MTI had the highest AUROC (0.987) for the detection of glioma recurrence.

Supplemental Data. On the basis of these data, the diagnostic performance metrics were as follows:

- cMRI: sensitivity 83.0%, specificity 93.8%, precision 98.3%, accuracy 85.1%, and F1 score 90.0%.
- μPerf: sensitivity 97.9%, specificity 95.1%, precision 98.8%, accuracy 97.4%, and F1 score 98.4%.

Quantitative imaging biomarker evaluation and ROC analysis (Fig 5) revealed that MTI had the highest AUROC (0.987; $P <$ .001; 95% CI, 0.976–0.999) for detecting glioma recurrence, followed closely by μCBV (AUROC = 0.982; $P <$ .001; 95% CI, 0.965–0.998) and CBV (AUROC = 0.941; $P <$ .001; 95% CI, 0.918–0.965), albeit with some separation.

The imaging biomarker values for cMRI (ie, macrovascular CBV) and μPerf (ie, μCBV and MTI) for the diagnostic subgroups are summarized in the Supplemental Data.

For FN findings in cMRI, CBV values were significantly lower ($P <$ .001) compared with TP findings and were not significantly different from TN and cNWM values. These results quantitatively confirmed that macrovascular perfusion, as measured in routine clinical settings, may not be elevated in early glioma recurrences.

For FP findings in cMRI, CBV values showed a considerable variability (2.3%–21%). Due to the small sample size ($n = 5$), no significant differences were observed relative to other subgroups.

For early TP findings in μPerf, both μCBV and MTI values were significantly elevated ($P <$ .001) compared with TN findings and cNWM but did not differ significantly from other TP results. These findings quantitatively confirm microvascular hyperperfusion and neovascularization in the early stages of glioma recurrence.

For FN finding in μPerf, glioma recurrences without increased μPerf, observed in 2 *IDH*-mutated astrocytomas WHO grade 2, one astrocytoma *IDH*-wild-type NOS, and 3 glioblastomas, exhibited significantly lower μCBV ($P <$ .01) and MTI ($P <$ .001) values compared with TP findings but were not significantly different from TN or cNWM. This result is noteworthy for glioblastomas, in which the absence of increased microperfusion and

neovascularization is unusual, with the underlying reasons remaining unclear.

Among the 4 FP cases for $\mu$Perf (3 glioblastoma, 1 oligodendroglioma WHO grade 3, *IDH*-mutant, 1p19q codeleted), $\mu$CBV and MTI values did not significantly differ from the those in the TP subgroup but were significantly distinct from cNWM ($P <$ .05). Although subtle, the signs of $\mu$Perf in these cases were significant, and their underlying cause remains unexplained. A possible explanation could be that $\mu$Perf is sensitive to an increase in microvessels that can occur as part of the wound healing effects in response to radiation therapy.

## DISCUSSION

Gliomas, particularly GBMs, as one of the most devastating cancers due to their infiltrative growth patterns, high recurrence rates, and poor prognosis, remain a critical challenge in clinical management despite aggressive treatment protocols urging early detection and intervention of tumor recurrence.[5] Conventional MRI techniques such as ceT1w MRI, DWI, or gradient-echo-based DSC perfusion MRI face limitations in distinguishing early recurrence from treatment-related changes like radiation necrosis, leading to diagnostic and therapeutic uncertainty and delay.

In this study, we evaluated the clinical utility of a microvascular perfusion imaging technique based on spin-echo MRI, which is designed to enhance MRI sensitivity in detecting early glioma recurrence by capturing capillary changes indicative of tumor-related neovascularization.

Our primary findings were 4-fold: 1) $\mu$Perf yielded superior diagnostic performance compared with cMRI in follow-up monitoring of patients with glioma; 2) $\mu$Perf facilitated the early detection of glioma recurrence; 3) $\mu$Perf complements routine clinical MRI protocols; and 4) early recurrences of gliomas with high-grade malignancy predominantly exhibit microvascular changes in contrast to advanced recurrences.

Recent literature indicates the evolving role of advanced cMRI techniques in glioma follow-up monitoring. For instance, perfusion MRI, particularly gradient-echo DSC MRI, has shown encouraging results in differentiating tumor progression from treatment-related changes in high-grade gliomas. Patel et al[19] reviewed 28 studies, reporting pooled sensitivities and specificities of 90% and 89%, respectively, for the best-performing parameters. DWI, including ADC mapping, showed a pooled sensitivity of 71% and specificity of 87%. The diagnostic parameters of cMRI in our study (sensitivity 83%, specificity 94%) are in line with these meta-analysis findings.

The recently updated RANO criteria (RANO 2.0)[20] highlighted the increasing interest in amino acid PET to predict tumor response and to distinguish pseudoprogression from progression. For example, Puranik et al[21] observed an overall diagnostic accuracy of 87.1% using [$^{18}$F]-fluoroethyl-tyrosine (FET) PET in a single-center multidisciplinary clinically-controlled study including 171 patients with high-grade gliomas, while Panholzer et al[22] reported an AUROC of 0.91 using tumor-to-brain FET-PET ratios in 37 patients with WHO grade 2–4 gliomas. Combining FET-PET with gradient-echo DSC MRI metrics (CBV and TTP) further improved the diagnostic performance, achieving an AUROC of 0.98. Our $\mu$Perf

approach showed comparable diagnostic parameters, with an accuracy of 97.4% and AUROCs of 0.987 and 0.982 for MTI and $\mu$CBV, respectively.

To our knowledge, no prior studies have compared the early detection capabilities of experimental MRI techniques with cMRI. Using $\mu$Perf, we were able to detect glioma recurrence earlier than cMRI in 13.5% of analyzed follow-up MRIs (57 of 422 examinations), within a timeframe ranging from 41 to 353 days (mean, 137 days). In the 35 cases in which the FN cMRI finding prevented early treatment of FNs in cMRI often lacked hyperperfusion (no increased CBV) in gradient-echo DSC MRI.

We demonstrated that gradient-echo DSC perfusion MRI alone is insufficient to detect early-stage glioma recurrence. Therefore, spin-echo-DSC perfusion MRI should be considered for future updates of the RANO criteria.[20] Furthermore, we showed that the $\mu$Perf technique integrates seamlessly with routine MRI protocols. Our study involved 2003 follow-up MRI examinations of 351 patients with glioma for 9 years. Including initial diagnoses and other types of brain tumors, the technique was used in 2800 MRI scans across 850 patients. This information demonstrates that the technique is compatible with cMRI protocols and requires only an additional 2 minutes for data acquisition. $\mu$CBV can be calculated directly from spin-echo DSC perfusion MRI data, comparable with the method for CBV, without requiring complex postprocessing software, illustrating its utility in clinical practice.

Our findings support the hypothesis that $\mu$Perf, with its enhanced sensitivity to microvascular changes, offers superior performance compared with cMRI in detecting glioma recurrence at an early stage. Tumor volumes small as 1–2 mm$^3$, apparent in early glioma recurrence, require a sufficient supply of oxygen and nutrients from neighboring capillaries via vascular co-option,[9] given that the diffusion distance of oxygen is 100–200 $\mu$m.[23] However, to grow beyond this size, the recruitment of de novo blood vessels toward the tumor, ie, neovascularization, is required.[24,25] Previous studies[26,27] have observed an increase in vessel diameters during GBM progression by using the cranial window technique in orthotopic mouse models. Our $\mu$Perf approach has the capability of detecting these newly formed vascular structures due to the high sensitivity of spin-echo DSC perfusion MRI for microvessels with diameters around 10 $\mu$m.

Despite the promising results, this study has several confounders that warrant consideration. A primary limitation is the retrospective nature of the data analysis, including biased patient selection and data interpretation, limiting the generalizability of the findings. While our sample size was substantial, certain patterns of recurrence or progression may not have been adequately captured, particularly in patients with an atypical disease courses or those undergoing experimental treatments. Further validation through multicenter studies is essential to enhance the generalizability of these results. Another limitation of our approach is its reliance on an additional DSC MRI perfusion sequence (spin-echo DSC) and a second contrast agent injection. However, this preserves the spatial and temporal resolution of routine gradient-echo DSC perfusion MRI sequence. Our protocol provides data acquisition with a high SNR and excellent spatial resolution across the entire brain, critical for MR perfusion examinations in

clinical settings, particularly in detecting small or multicentric lesions. Unfortunately, the alternative simultaneous gradient-echo spin-echo DSC perfusion sequence still has certain disadvantages in terms of spatial resolution and coverage,[28-33] so the further development of this technique should be encouraged. The spin-echo-DSC technique has a much lower SNR compared with the gradient-echo DSC technique, and how noise and contrast-to-noise ratio affected the estimations of vascular parameters was not considered in this study. Digernes et al[34] showed that a low contrast-to-noise ratio led to overestimations of CBV and underestimations of the vortex area. This result could potentially affect the clinical interpretation of DSC-MRI and should, therefore, be taken into account in the clinical decision-making process.

Furthermore, our method is constrained by the complexity of interpreting imaging biomarkers such as MTI, which require sophisticated processing techniques that may not be universally accessible in all clinical settings. Although custom-made software and specialized algorithms enabled high-resolution data analysis, standardizing these techniques across different institutions and manufacturers remains challenging. Last-, while the study provides strong evidence for the utility of $\mu$Perf in detecting glioma recurrence earlier than cMRI, it does not correlate the potential impact of earlier detection on long-term patient outcomes, such as survival rates and/or quality of life.

The implications of this study for patient care might be significant. By improving early detection of glioma recurrence through advanced imaging techniques like $\mu$Perf, clinicians can make more informed decisions regarding the time point of treatment interventions, permitting the conceptualization of personalized management strategies tailored to individual patient needs. Future research should focus on exploring the integration of $\mu$Perf with other advanced imaging modalities such as amino acid PET or leveraging machine learning algorithms to provide a more holistic approach across different biophysical properties in clinical glioma management. Longitudinal studies examining the relationship between early vascular changes detected by $\mu$Perf and long-term patient outcomes would be beneficial in establishing a framework on how to integrate $\mu$Perf in routine practice.

## CONCLUSIONS

Our findings support the hypothesis that $\mu$Perf, leveraging microvascular perfusion imaging, enhances early detection of glioma recurrence, outperforming cMRI techniques. The $\mu$Perf method demonstrated superiority due to its diagnostic capabilities, capturing subtle vascular changes indicative of tumor neovascularization. This approach addresses relevant unresolved issues in glioma management by detecting early-stage vascular alterations associated with recurrence. Additionally, $\mu$Perf is compatible with routine clinical follow-up protocols, requiring an additional 2 minutes for data acquisition, making it useful for widespread clinical implementation. Although promising, further validation and research related to the long-term impact on survival and quality of life are necessary to support broader clinical adoption and integration with other advanced imaging modalities.

Disclosure forms provided by the authors are available with the full text and PDF of this article at www.ajnr.org.

## REFERENCES

1. Wen PY, Weller M, Lee EQ, et al. **Glioblastoma in adults: a Society for Neuro-Oncology (SNO) and European Society of Neuro-Oncology (EANO) consensus review on current management and future directions.** *Neuro Oncol* 2020;22:1073–113 CrossRef Medline

2. Mendez JS, Ostrom QT, Gittleman H, et al. **The elderly left behind-changes in survival trends of primary central nervous system lymphoma over the past 4 decades.** *Neuro Oncol* 2018;20:687–94 CrossRef Medline

3. Marko NF, Weil RJ. **The molecular biology of WHO grade II gliomas.** *Neurosurg Focus* 2013;34:E1 CrossRef Medline

4. Poon MT, Sudlow CL, Figueroa JD, et al. **Longer-term (≥ 2 years) survival in patients with glioblastoma in population-based studies pre- and post-2005: a systematic review and meta-analysis.** *Sci Rep* 2020;10:11622 CrossRef Medline

5. Perrini P, Gambacciani C, Weiss A, et al. **Survival outcomes following repeat surgery for recurrent glioblastoma: a single-center retrospective analysis.** *J Neurooncol* 2017;131:585–91 CrossRef Medline

6. Tsakiris C, Siempis T, Alexiou GA, et al. **Differentiation between true tumor progression of glioblastoma and pseudoprogression using diffusion-weighted imaging and perfusion-weighted imaging: systematic review and meta-analysis.** *World Neurosurg* 2020;144: e100–09 CrossRef Medline

7. Schmiedeskamp H, Straka M, Newbould RD, et al. **Combined spin- and gradient-echo perfusion-weighted imaging.** *Magn Reson Med* 2012;68:30–40 CrossRef Medline

8. Boxerman JL, Hamberg LM, Rosen BR, et al. **MR contrast due to intravascular magnetic susceptibility perturbations.** *Magn Reson Med* 1995;34:555–66 CrossRef Medline

9. Hardee ME, Zagzag D. **Mechanisms of glioma-associated neovascularization.** *Am J Pathol* 2012;181:1126–41 CrossRef Medline

10. Louis DN, Perry A, Wesseling P, et al. **The 2021 WHO Classification of Tumors of the Central Nervous System: a summary.** *Neuro Oncol* 2021;23:1231–51 CrossRef Medline

11. Essig M, Wenz F, Scholdei R, et al. **Dynamic susceptibility contrast-enhanced echo-planar imaging of cerebral gliomas: effect of contrast medium extravasation.** *Acta Radiol* 2002;43:354–59 CrossRef Medline

12. Boxerman JL, Prah DE, Paulson ES, et al. **The role of preload and leakage correction in gadolinium-based cerebral blood volume estimation determined by comparison with MION as a criterion standard.** *AJNR Am J Neuroradiol* 2012;33:1081–87 CrossRef Medline

13. Welker K, Boxerman J, Kalnin A, et al; American Society of Functional Neuroradiology MR Perfusion Standards and Practice Subcommittee of the ASFNR Clinical Practice Committee. **ASFNR Recommendations for Clinical Performance of MR Dynamic Susceptibility Contrast Perfusion Imaging of the Brain.** *AJNR Am J Neuroradiol* 2015;36:E41–51 CrossRef Medline

14. Stadlbauer A, Zimmermann M, Heinz G, et al. **Magnetic resonance imaging biomarkers for clinical routine assessment of microvascular architecture in glioma.** *J Cereb Blood Flow Metab* 2017;37:632–43 CrossRef Medline

15. Bjørnerud A, Emblem KE. **Method for quantitative cerebral hemodynamic analysis using DSC–MRI.** *J Cereb Blood Flow Metab* 2010;30:1066–78 CrossRef Medline

16. Stadlbauer A, Zimmermann M, Oberndorfer S, et al. **Vascular hysteresis loops and vascular architecture mapping in patients with glioblastoma treated with antiangiogenic therapy.** *Sci Rep* 2017;7: 8508 CrossRef Medline

17. Ducreux D, Buvat I, Meder JF, et al. **Perfusion-weighted MR imaging studies in brain hypervascular diseases: comparison of arterial input function extractions for perfusion measurement.** *AJNR Am J Neuroradiol* 2006;27:1059–69 Medline

18. Stadlbauer A, Zimmermann M, Kitzwögerer M, et al. **MR imaging–derived oxygen metabolism and neovascularization characterization for grading and IDH gene mutation detection of gliomas.** *Radiology* 2017;283:799–809 CrossRef Medline

19. Patel P, Baradaran H, Delgado D, et al. **MR perfusion-weighted imaging in the evaluation of high-grade gliomas after treatment: a systematic review and meta-analysis.** *Neuro Oncol* 2017;19:118–27 CrossRef Medline

20. Youssef G, Wen PY. **Updated Response Assessment in Neuro-Oncology (RANO) for gliomas.** *Curr Neurol Neurosci Rep* 2024;24:17–25 CrossRef Medline

21. Puranik AD, Dev ID, Rangarajan V, et al. **FET PET to differentiate between post-treatment changes and recurrence in high-grade gliomas: a single center multidisciplinary clinic controlled study.** *Neuroradiology* 2025;67:363–69 CrossRef Medline

22. Panholzer J, Malsiner-Walli G, Grün B, et al. **Multiparametric analysis combining DSC-MR perfusion and [$^{18}$F]FET-PET is superior to a single parameter approach for differentiation of progressive glioma from radiation necrosis.** *Clin Neuroradiol* 2024;34:351–60 CrossRef Medline

23. Katayama Y, Uchino J, Chihara Y, et al. **Tumor neovascularization and developments in therapeutics.** *Cancers (Basel)* 2019;11:316 CrossRef Medline

24. Folkman J, Kalluri R. **Cancer without disease.** *Nature* 2004;427:787 CrossRef Medline

25. Carmeliet P, Jain RK. **Angiogenesis in cancer and other diseases.** *Nature* 2000;407:249–57 CrossRef Medline

26. D'Alessandris QG, Pacioni S, Stumpo V, et al. **Dilation of brain veins and perivascular infiltration by glioblastoma cells in an in vivo assay of early tumor angiogenesis.** *Biomed Res Int* 2021;2021:8891045 CrossRef Medline

27. Mathivet T, Bouleti C, Van Woensel M, et al. **Dynamic stroma reorganization drives blood vessel dysmorphia during glioma growth.** *EMBO Mol Med* 2017;9:1629–45 CrossRef Medline

28. Sorensen AG, Batchelor TT, Zhang WT, et al. **A "Vascular Normalization Index" as potential mechanistic biomarker to predict survival after a single dose of cediranib in recurrent glioblastoma patients.** *Cancer Res* 2009;69:5296–300 CrossRef Medline

29. Kiselev VG, Strecker R, Ziyeh S, et al. **Vessel size imaging in humans.** *Magn Reson Med* 2005;53:553–63 CrossRef Medline

30. Emblem KE, Mouridsen K, Bjornerud A, et al. **Vessel architectural imaging identifies cancer patient responders to anti-angiogenic therapy.** *Nat Med* 2013;19:1178–83 CrossRef Medline

31. Schmainda KM, Rand SD, Joseph AM, et al. **Characterization of a first-pass gradient-echo spin-echo method to predict brain tumor grade and angiogenesis.** *AJNR Am J Neuroradiol* 2004;25:1524–32 Medline

32. Batchelor TT, Gerstner ER, Emblem KE, et al. **Improved tumor oxygenation and survival in glioblastoma patients who show increased blood perfusion after cediranib and chemoradiation.** *Proc Natl Acad Sci U S A* 2013;110:19059–64 CrossRef Medline

33. Eichner C, Jafari-Khouzani K, Cauley S, et al. **Slice accelerated gradient-echo spin-echo dynamic susceptibility contrast imaging with blipped CAIPI for increased slice coverage.** *Magn Reson Med* 2014;72:770–78 CrossRef Medline

34. Digernes I, Nilsen LB, Grøvik E, et al. **Noise dependency in vascular parameters from combined gradient-echo and spin-echo DSC MRI.** *Phys Med Biol* 2020;65:225020 CrossRef Medline